IEEE Access
Multidisciplinary ⋮ Rapid Review ⋮ Open Access Journal

Received 7 September 2023, accepted 29 September 2023, date of publication 6 October 2023, date of current version 12 October 2023.

Digital Object Identifier 10.1109/ACCESS.2023.3322651

RESEARCH ARTICLE

Real-Time State of Charge Estimation of Light Electric Vehicles Based on Active Power Consumption

MARCO PASETTI[1], (Member, IEEE), SALVATORE DELLO IACONO[1], (Member, IEEE), AND DARIO ZANINELLI[2], (Senior Member, IEEE)

[1]Department of Information Engineering, Università degli Studi di Brescia, 25123 Brescia, Italy
[2]Department of Energy, Politecnico di Milano, 20156 Milan, Italy

Corresponding author: Marco Pasetti (marco.pasetti@unibs.it)

This work was supported in part by the Centro Nazionale per la Mobilità Sostenibile (MOST)—Sustainable Mobility National Research Center; and in part by the European Union (EU) Next-Generation EU through (Piano Nazionale di Ripresa e Resilienza (PNRR)—MISSIONE 4 COMPONENTE 2, INVESTIMENTO 1.4—D.D. 1033 17/06/2022, CN00000023), Spoke 5 "Light Vehicle and Active Mobility" and Spoke 13 "Electric Traction Systems and Batteries."

ABSTRACT Battery state of charge estimation is not new, and the literature is rich in examples. Still, in most cases, state of charge algorithms are embedded in battery chargers and do not present the charging stage with a standard communication form, thus limiting the possibility of applying advanced smart charging algorithms. To overcome this limitation, this study proposes a method for the estimation of the state of charge of onboard batteries installed on light electric vehicles and the identification of their charging stage, if charged by the constant-current/voltage method, without the need for direct current measurements or communication from the light electric vehicle battery management system. The method is based on a preliminary off-line characterization of the full charge of a given battery/charger set by implementing a learning algorithm. The parameters learned during the off-line test are then used in on-line applications to estimate the light electric vehicle's state of charge and identify its charging stage by only using the active power measured at the light electric vehicle charging socket. The method was tested on two different instances of the same battery/charger set family installed on two different light electric vehicles, providing a state of charge estimation with an overall accuracy of about 1.5%, computed as root mean square error over the whole state of charge range. The results showed that the proposed method could be successfully applied to estimate the real-time state of charge of light electric vehicles by only using low-cost electronic devices.

INDEX TERMS Charging state identification, state of charge estimation, light electric vehicles, smart charging, power demand.

I. INTRODUCTION

Light Electric Vehicles (LEVs), such as electric bikes (or e-Bikes) are becoming more popular, along with other electric modes of sustainable transportation, profiting from the rising sustainability needs, health consciousness, and pollution awareness in society. While global electric car sales touched 10 million in 2020, in the same year LEVs counted about 25 million devices [1]. LEVs have high market shares, especially in Asia: China recorded an increase in sales of about 25 % per year from 2015 to 2021, while in the European Union LEVs reached in 2021 the 5 % share of the global Electric Vehicle (EV) market [2]. Several concerns, however, have been raised about the impact of EVs on the operation of power grids; many studies observed that if the majority of EVs are charged at grid peak time, their increasing penetration could sensibly affect distribution grids.

The literature is rich in studies on the impact of EVs on power grids, as reported in [3], [4], and [5], just to mention a few, but none of these studies focuses on the impact of

The associate editor coordinating the review of this manuscript and approving it for publication was Salvatore Favuzza.

LEVs, despite their increasing penetration on the market. Indeed, LEVs are generally reputed to be less challenging than EVs, as the stored energy and peak consumption of LEVs is considerably lower than EVs; however, LEVs suffer from the same problem of charge port standardization and charge methods. In fact, in order to maintain low-cost high manufacturing volumes, LEV chargers are commonly made with low-efficiency Alternating Current (AC) to Direct Current (DC) power converters, with fewer protection and lower power factors compared to the state-of-art devices. More efficient charging systems, such as DC charging, are appearing on the market, but even though DC charging for e-Bikes is already a reality, it is still manufacturer-specific and no standardization exists for connectors and communications [6].

Besides the power electronics components and standardization issues, one of the major problems of LEV stations is related to the quality of the service provided to final users. If security concerns are neglected, the quality of service perceived by final users can be represented by two simple questions that a typical user could rise: (1) there will be any free power outlet to charge my bike? (2) will be the bike charged according to my needs?

When looking for a charging station during a trip or when reaching a parking lot, the availability of power outlets is the main concern. Conversely, when picking up their bike, the main concern of users is about the State of Charge (SoC) of onboard batteries. Indeed, users have only a rough estimate of the time required to charge their devices, and they tend to keep their bikes plugged into power outlets for longer times than required, since they don't (typically) have a real-time estimation of the battery SoC.

On the other hand, when considering the perspective of service providers, i.e., Charge Point (CP) operators, the ability of providing a high quality service is mainly related to the ability of serving the highest number of users with the desired recharge level, at the lowest cost, and at the highest sustainability grade. Indeed, the use of renewable energy, mainly from Photovoltaic (PV) systems, both in EV and LEV charging stations, installed in extra-urban contexts (e.g., tourist cycle routes), is considered an attractive solution [7]. In such systems, particularly in the case of grid-tied installations, the minimization of the carbon footprint requires the adoption of scheduling and modulation techniques (usually referred as smart charging) able to maximize the self-consumption of the renewable source [8].

A. AIM AND MAJOR CONTRIBUTIONS

As detailed in the literature analysis provided in Section II, even though smart charging approaches are appearing in the literature, the effective implementation of these strategies requires the real-time estimation the SoC of onboard batteries. However, all the studies in the literature assumed that the SoC is known *a priori* or it is provided by the user or by means of machine-to-machine communication between the Battery Management System (BMS) onboard the vehicle and the charging station, which is not usually implemented in real-world applications.

The current standard for LEV charging (i.e., the IEC 61851 Mode 1 [9]) does not provide a specific communication and charging protocol. As a consequence, all commercial vehicles have their own battery/BMS/charger set that depends on the specific manufacturer implementation and usually does not allow external communication.

This study aims to overcome the limitations due to the missing standardization in the communication interface for battery chargers and CP management systems by proposing a novel method for the real-time estimation of the SoC and charging stage of LEVs. In particular, the study proposes a method which is independent from DC measurements or internal BMS communication, and only requires the use of low-cost smart meters measuring the AC active power delivered by the electrical sockets of conventional LEV charging stations. The proposed method is able to:

1) estimate the LEV SoC while charging by only accessing the AC active power measured at the electrical charging socket;
2) identify and classify the charging stage of the LEV, i.e., the Constant Current (CC) mode, the Constant Voltage (CV) mode, the End of Charge (EoC), and the Charge-Keeping (CK) mode;
3) estimate the remaining time to reach a desirable SoC.

The proposed method can be applied to all the chargers implementing the Constant-Current Constant-Voltage (CCCV) charging scheme, i.e., the charging method implemented in the majority of LEV chargers available on the market. Starting from a preliminary Off-Line characterization of the full charge of a given LEV battery/BMS/charger set by means of AC and DC measurements, the method can be applied in On-Line applications to estimate the charging stage and SoC of the LEV by only using the AC active power measured at the LEV charging socket.

B. ARTICLE ORGANIZATION

In Section II, starting from the classical definition of battery state of charge, the classification of literature methods and models used for the estimation of the SoC of LEV batteries is reported, by also discussing battery charging methods and smart charging strategies. Section III provides the description of the proposed method, starting from the general overview to the detailed description of the charging stage identification and real-time SoC estimation algorithms and models. In Section IV the measurement setup used during the execution and validation of the presented method is reported, while the results and discussion of the experiments are reported in Section V. Finally, Section VI summarizes the conclusions of the study and discusses its potential applications.

II. LITERATURE REVIEW

A. SOC ESTIMATION METHODS

State of charge definition is not unique and can express the charge that is present or the portion of energy that the user can withdraw from the battery under the working conditions. It can mathematically defined as in (1):

$$SoC(t) = \frac{Q(t)}{Q_n}, \tag{1}$$

where $Q(t)$ is the current battery capacity, and Q_n is the nominal capacity given by the manufacturer and represents the maximum amount of charge that can be stored in the battery. Thus, the problem of the SoC identification and estimation arises.

The simplest method that can be used to estimate the battery SoC is called the "Coulomb Counting Method", also known as Ah counting (AHC). AHC is the conventional method to estimate the SoC and results in direct relationship between the battery current and the SoC, and, as introduced by [10], it can be calculated as:

$$SoC(t) = SoC(t_0) + \frac{1}{Q_n}\int_{t_0}^{t} \eta i(t)dt, \tag{2}$$

where:

- $SoC(t)$ is the battery state of charge at time t,
- $SoC(t_0)$ is the initial state of charge (i.e., the state of charge at time t_0),
- η is the coulombic efficiency, describing the ratio between the energy change in the battery and that spent to store the charges or that provided by the charges during the charging or discharging process, respectively,
- $i(t)$ is the battery current at time t.

Despite its low computational complexity, which makes the AHC attractive for embedded applications, the accuracy of the Coulomb counting method depends on many factors, mainly: the accuracy of the battery current measurement, the estimation of the initial $SoC(t)$ value, the accuracy of current sensors, and the stability of the measurement process [11]. Moreover, being an open loop method, coulomb counting is subject to accumulation uncertainty effects due to the integrative nature of the measurement, which could lead to significative global uncertainties.

Even though SoC gauges appeared since the beginning of battery usage as battery voltage meters, the SoC evaluation is still a discussed problem, and the literature is rich in examples. The classification of SoC estimation methods is not unique in literature, but in general it is divided according to the type of model underlying the evaluation of the SoC and State of Health (SoH). In Fig. 1 a schematic representation of different SoC estimation approaches is reported; as it can be seen, three main categories can be identified [12]: model-based approaches, sensor-based, and data-driven (or algorithm-based) SoC identification.

1) SENSOR-BASED METHODS

Sensor-based SoC identification is relatively new and is the less common approach; different in-situ techniques have been used to directly probe the physical states of the battery, for example, X-ray diffraction, neutron imaging, and electrochemical impedance spectroscopy. More recent techniques for lithium-ion batteries involve ultrasonic guided wave canning [13], [14], [15] or using piezoelectric actuators to stimulate cells and sensors to measure changes in time of flight. All these techniques have in common that they are difficult to practically implement and, in most cases, can only be performed in the laboratory.

2) MODEL-BASED METHODS

Model-based SoC identification estimates the battery state of charge by using an analytical battery model with different degrees of precision and accuracy. The two most common battery models are Electrochemical Modelling (ECM), which explicitly represents in detail the chemical processes that take place in the battery, and Equivalent Electrical Circuit Models (EECM). ECMs are mainly based on Nernst's theory and the Butlere-Volmer, and one of the most popular and early approaches is a lumped parameter model that describes the battery with a series of differential-algebraic equations [16]. These have been used to describe lead-acid and non-rechargeable batteries, but they are insufficient to describe complex electrochemical processes happening in modern batteries technologies, such as lithium-ion, for which porous electrode and concentrated solution theories are required [17], [18]. EECM techniques abstract away the physical nature of the battery and try to represent it with circuital models, resulting in a simpler computation. These models use classic circuit theory lumped linear (resistor, capacitor, controlled voltage, and current source) and non-linear components (diodes) to describe the battery characteristic.

Electrochemical Impedance Spectroscopy (EIS) is widely used as a measurement method to obtain electrochemical impedance models on a wide range of frequencies [19]. Being a non-destructive method, EIS is used in battery production to evaluate the complex impedance spectrum of lithium batteries that is directly correlated with its SoC and SoH, but despite its accuracy, it is not suitable for online parameterization due to long test time required.

3) DATA-DRIVEN METHODS

Data-driven methods (DDM) are different from the previously described approaches because they limit the need for an analytical description of the battery making in favour of statistical tools such as Artificial Neural Networks (ANN), fuzzy logic, support vector machines, genetic algorithms, and others machine learning tools to estimate the SoC [20]. They use voltage, current, and temperature signals to evaluate the battery SoC thanks to the training on numerous data at different battery conditions. This approach results in a

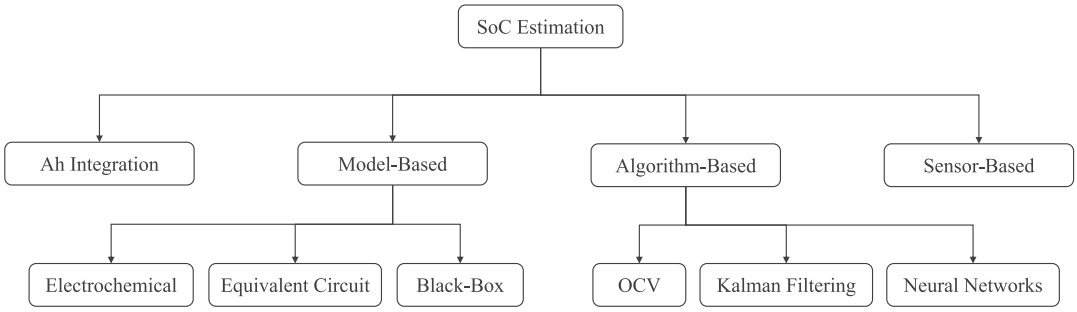

FIGURE 1. State of charge estimation approaches according to the adopted battery model.

black-box that can be used for online SoC estimation, but with the main disadvantage being the immense data-set and time-consuming training required to cover all the possible operating conditions.

The Open Circuit Voltage (OCV) method can be classified between DDMs [21], [22], this technique is difficult to apply for online SoC estimation due to the measurement precision required and the long relaxation time to achieve charge and discharge equilibrium conditions.

4) ADAPTIVE AND HYBRID METHODS

There is a plethora of adaptive and hybrid methods presented in the literature that combine the classical approaches based on OCV, AHC, or their combination with ANNs [23] and Convolutional Neural Netwotks [24], to obtain the best results in terms of SoC estimation accuracy and to estimate the battery SoH ans Remaining Usefoul Life [25]. They have been successfully used in order to obtain real-time battery temperature estimation for fault diagnosis [26].

In the domain of battery model-based estimation, Linear Kalman Filters and Non-Linear Kalman Filters [27], [28] are widely used thanks to their improved accuracy, robustness, their suitability for online estimation, and the possibility of co-estimation for SoC and battery parameters such as the battery capacity [29], [30]. Dual Fractional-order Extended Kalman Filter have been employed to estimate lithium-ion battery's states and parameters with constant phase element in order to describe chemical process within porous electrodes [26]. Finally, hybrid approaches that combine features of a physics-based model, filtering methods such as Extended Kalman Filter, Unscented Kalman Filter, and Unscented Particle Filter, and Artificial Intelligence exist, and they are successfully used for estimating the State of Health and applying condition monitoring of lithium-ion battery [31].

B. CHARGE METHODS

Depending on the chemical structure of the cells, the charging profiles of batteries can be quite different from each other. The most commons for Li-Ion batteries are the pulse charging scheme and the CCCV charging scheme [32].

The first one, despite its simplicity and low number of required electrical components, has major disadvantages due to the high-peak current pulses in the battery that provoke high voltage at battery terminals that can be higher than its maximum rated voltage, being quite hazardous and causing damages, especially to Li-Ion batteries. On the other hand, the CCCV charging scheme is more complex to implement because it involves multiple phases: trickle, constant-current and constant-voltage. This charging scheme can be implemented in different electronic topologies; linear, being the simpler, or switching, being smaller and more efficient but with possible electro-magnetic compatibility issues.

Other solutions exist, like the five-step charging pattern that consists in a multistage constant-current charging method [33]. Most of the solutions make use of the battery SoC in order to choose the correct charging strategy and current value or to limit the battery degradation by means of a BMS.

C. SMART CHARGING STRATEGIES

To implement the optimal management of charging stations, in both terms of energy/CO_2 flows and quality of service, CP operators need to manage the amount of energy delivered to each user and optimize the energy consumption from available sources. To reach these goals, different charge strategies, usually referred as smart charging, have been proposed in the literature.

Examples of smart charging stations with PV for LEVs are appearing in the literature [6], [34], and strategies for charging LEVs are proposed to maximize the use of renewable energy and balance the available energy with the demand of the individual vehicle [35]. In the case of the charging stations proposed in [34], PV energy was managed with a first-order objective to minimize the consumption from the grid. However, due to the lack of standard communication with the LEV internal Battery Management System (BMS), missing or excess solar energy was supposed to be exchanged with the grid.

The authors in [36] proposed a general probabilistic model for the charge decision of EVs as a function of the battery SoC and the required daily range to compute the

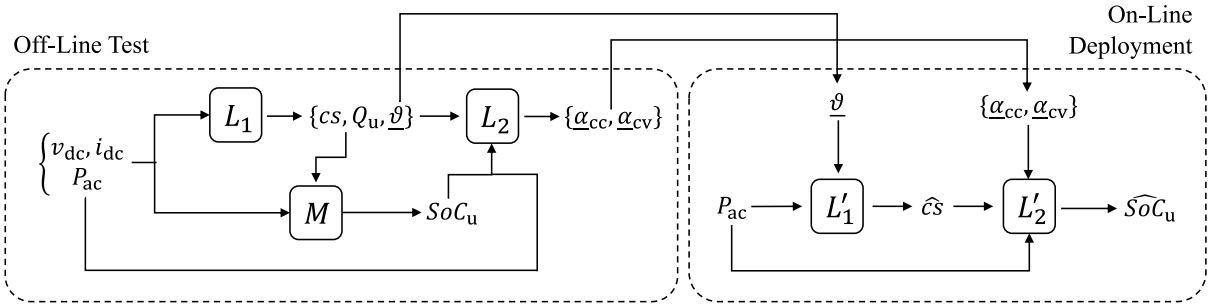

FIGURE 2. Block diagram of the proposed method.

charging needs from the point of view of the grid. The study was performed by introducing the definition of the steady-state SoC level as the distribution of SoC levels across an entire EV fleet. A charge decision problem was developed based on a well-defined probability distribution function and then used to simulate the energy requirements associated with the complete electrification of cars of a real-world scenario (i.e., for the city of Frederiksberg, Denmark).

In [37], authors investigated two smart charging strategies for LEVs (i.e., an e-scooter with a power of 2 kW and an energy consumption of 3 kWh per 100 km): one based on a grid-connected PV system and the second one with a battery storage system. In both systems, the user was required to specify the initial SoC and the expected duration of the parking time. The smart strategies were then designed with the aim of increasing the self-consumption of the PV to reduce the amount of energy absorbed from the grid.

III. PROPOSED METHOD

The proposed method is based on two different stages, namely the Off-Line test and the On-Line deployment. Let's define:

Battery/Charger Set (BCS) the set formed by a battery pack, its BMS, and related charger. The BCS is formed by a combination of battery pack (i.e., as combination of batteries and their BMS) and charger model provided by a specific manufacturer, and represents the class of devices (i.e., represented by a manufacturer and model) that is characterized during the Off-Line stage;

Off-Line Test it refers to the stage deployed in testing (i.e., laboratory) conditions where the considered BCS undergoes a full charge test to produce a training set of AC and DC measurements. The combination of AC and DC measurements is used by the learning algorithm L_1 to derive the charging stage cs, the related set of $\underline{\vartheta}$ parameters, and to compute the charged capacity ΔQ. The charging stage cs, the charged capacity ΔQ, and the DC measurements are then used to estimate the usable SoC profile of the battery under test, namely SoC_u, by applying the SoC measuring method M. Finally, the charging stage cs information and the AC measurements are used by the learning algorithm L_2 to compute the set of regression parameters $\{\underline{\alpha}_{cc}, \underline{\alpha}_{cv}\}$ of SoC_u;

On-Line Deployment it refers to the stage deployed in operating conditions, i.e., when the LEV is plugged into the charging socket. The proposed method assumes that the LEV is equipped with an instance of the BCS class (i.e., same model but different physical device) whose parameters $\underline{\vartheta}$, $\underline{\alpha}_{cc}$, and $\underline{\alpha}_{cv}$ have been learned during the Off-Line test. During the On-Line deployment, the charging stage $\widehat{cs}$ of the LEV is first identified by applying L'_1 over the AC active power consumption P_{ac} measured at the charging socket, and then $\widehat{SoC}_u$ is obtained by applying L'_2 over P_{ac} using $\underline{\alpha}_{cc}$ and $\underline{\alpha}_{cv}$.

The proposed method is summarized by the block diagram of Fig. 2, where:

- v_{dc} and v_{dc} are the DC voltage and current measurements at the terminals of the battery, respectively;
- P_{ac} is the active power consumption of the battery charger;
- the block M represents the SoC_u measuring model;
- L_1 and L_2 represent the charging stage cs and the SoC_u regression model identification algorithm, respectively;
- $\underline{\vartheta}$ and $\{\underline{\alpha}_{cc}, \underline{\alpha}_{cv}\}$ are the estimation parameters for cs and SoC_u, respectively;
- Q_u is the usable charging capacity.

In the following, the Off-Line Test and the On-Line Deployment are described in detail. First, the Off-Line Test is presented in Section III-A, including the description of the SoC_u measuring method M, the charging stage cs identification algorithm (L_1), and the SoC_u regression model (L_2). Second, the On-Line Deployment is described in Section III-B, including the description of the algorithm L'_1 used for the estimation of $\widehat{cs}$, and the algorithm L'_2 used for the estimation of $\widehat{SoC}_u$.

A. OFF-LINE TEST

Since the aim of this study is to asses the SoC a LEV battery in operating conditions for user-oriented applications, the reference state of charge considered in the proposed model is that perceived by the end user (in the following SoC_u). Indeed, a value of SoC_u can be defined against the the real state of charge of a battery (in the following SoC), as consequence of the control functions applied by the BMS during both the charge and discharge. The difference between these two

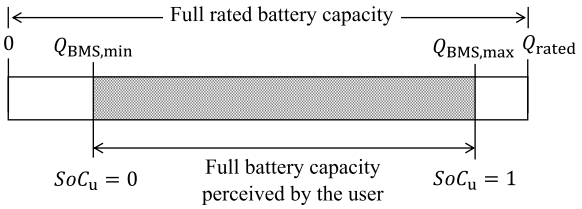

FIGURE 3. Representation of the meaning of the user state of charge SoC_u.

quantities is caused by the presence of the BMS that adapts the usable battery SoC range (i.e., SoC_u) to parameters like temperature and battery aging, in order to maintain a safe and healthy operation. The comparison between SoC_u and SoC is briefly depicted in Fig. 3, where $Q_{BMS,min}$ and $Q_{BMS,max}$ correspond to the minimum and maximum battery charge values allowed by the BMS, respectively.

During the Off-Line test the user state of charge SoC_u is measured by applying the measuring method M. In order to obtain a data set that would allow the identification of the expected charging stage $\widehat{cs}$ and state of charge $\widehat{SoC}_u$ over the full SoC_u range, the BCS undergoes a full charging test. Before the execution of the Off-Line test, the battery is discharged by riding the LEV up to the condition where no more power is delivered to the motor. In this case, corresponding to the $Q_{BMS,min}$ of Fig. 3, the SoC_u value can be assumed to be 0.

Once the battery has been (almost) fully discharged, i.e., up to a value of $SoC_u = 0$, the battery is connected to its charger and plugged into an AC outlet. Hence the battery is charged up to $Q_{BMS,max}$, i.e., up to $SoC_u = 1$.

To determine when $Q_{BMS,max}$ is reached, the identification of the charging stage corresponding to the End-of-Charge (EoC) is required. This identification (along with that of other charging stages and related parameters) is performed by the algorithm L_1 described in section III-A1.

1) CHARGING STAGE IDENTIFICATION

In this study it is assumed that the BMS of the BCS under test implements the CCCV charging scheme described in Section II-B. Based on this assumption, the following states, each identified by a charging stage value cs (being cs an integer ranging from 0 to 5), are assumed as representative of the finite state machine implemented by the BMS.

- Constant Current (CC) mode;
- Constant Voltage (CV) mode;
- Charge-Keeping (CK) mode.

In addition to the BMS states listed above, the following charging stages have been also introduced:

- Unknown Mode;
- Current to Voltage (CC2CV);
- End-of-charge (EoC).

It is worth noting that CC2CV and EoC represent transitory stages, i.e., corresponding to the transition from CC to CV, and from CV to CK, respectively. These stages are used by the cs identification algorithm L_1, while the Unknown Mode is only used by the cs estimation counterpart algorithm L_1'. The correspondence between the charging stages and their cs values is reported in Table 1.

TABLE 1. Charging stages enumeration.

cs	Description
0	Unknown
1	Constant Current (CC)
2	Current to Voltage (CC2CV)
3	Constant Voltage (CV)
4	End-of-Charge (EoC)
5	Charge-Keeping (CK)

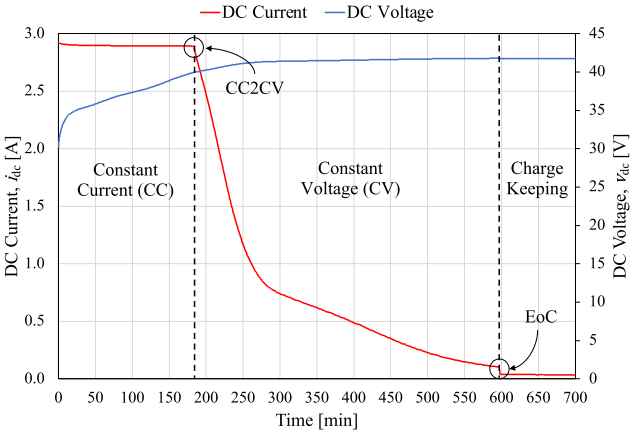

FIGURE 4. Representation of the CCCV charging stages during a full charge test, as combined information of the DC current i_{dc} and voltage curves v_{dc}.

An example of the charging stages listed above is depicted in Fig. 4, showing the DC voltage v_{dc} and current i_{dc} measurements recorded during the Off-Line test described in Section V. As it can be noted, the CC and CV stages can be easily identified by the changes in the charging current curve, which is a decreasing monotonic function with respect to the time. However, the small variations recorded during the CC stage and current measurement uncertainties could represent an issue for an automated identification algorithm.

On the other hand, the charging stage identification could be easier applied by using the DC power curve and power deviations, as depicted in Fig. 5, that shows the moving average of the DC power $\overline{p}_{dc}$ and the DC power average gradient Δp_{dc} during the same test represented of Fig. 4. Indeed, it can be noted that during the CC stage the DC power is an increasing monotonic function with respect to the time, while after the CC to CV transition the curve is a decreasing monotonic function. That means the CC to CV transition, being a cusp in the power function, can be easily

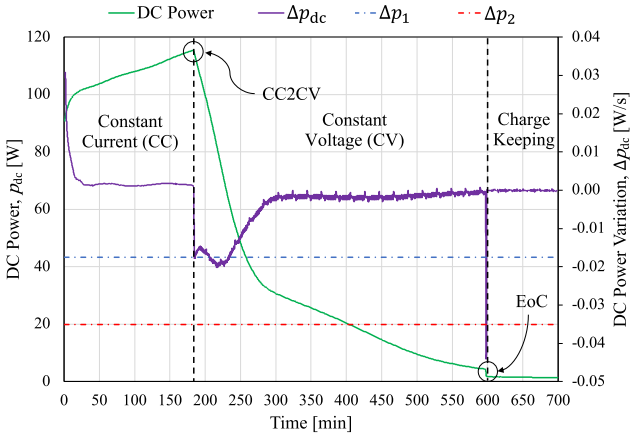

FIGURE 5. Representation of the CCCV charging stages during a full charge test, as combined information of the moving average of the DC power $\overline{p}_{dc}$ and the DC power average variation Δp_{dc}.

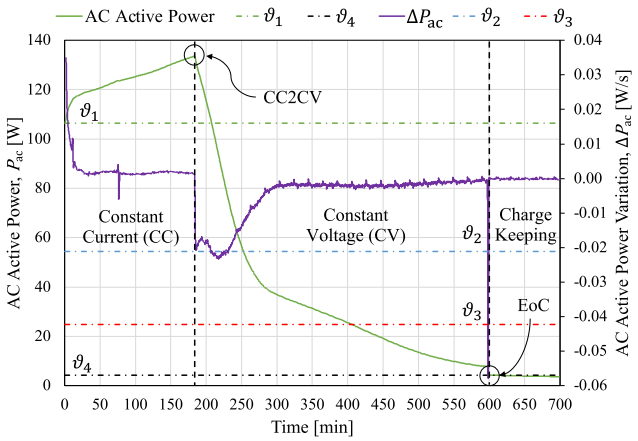

FIGURE 6. Representation of the CCCV charging stages during a full charge test, as combined information of the moving average of the AC active power $\overline{P}_{ac}$ and the DC power average variation ΔP_{ac}.

found by looking for a negative change in the Δp_{dc} function (denoted as Δp_1 in Fig. 4). Similarly, the CV to EoC transition corresponds to a rapid (also negative) change in the Δp_{dc}, that is at least two time greater than that recorded during the CC to CV transition. According to this observations, Δp_1 represents the change of power measurement corresponding to the CC to CV transition, while $\Delta p_2 = 2\Delta p_1$ is the threshold value corresponding to the CV to EoC transition.

Characteristics similar to those of the DC charging power curves of Fig. 5 can be found in the active power measurements, as depicted in Fig. 6, that shows the moving average of the AC power $\overline{P}_{ac}$ and the AC power average gradient ΔP_{ac} during the same test of Figs. 4 and 5.

In particular, when looking at the AC active power measurements of Fig. 6, power variations thresholds similar to Δp_1 and Δp_2 can be found, named ϑ_2 and ϑ_3, respectively. Furthermore, two additional parameters can be identified, i.e, the minimum AC active power recorded during the CC stage and at the end of the CV to EoC transition, named ϑ_1 and ϑ_4,

TABLE 2. Off-Line Test $\underline{\vartheta}$ parameters.

Parameter	Description
ϑ_1	Minimum AC active power recorded during the CC stage
ϑ_2	CC to CV threshold of AC active power variation
ϑ_3	CV to EoC threshold of AC active power variation
ϑ_4	Minimum AC active power recorded at the end of the CV to EoC transition

respectively. These parameters (summarized in table Table 2) are used to estimate the charging stage $\widehat{cs}$ during the On-Line Deployment by applying the L_1' algorithm.

Given:

- k: the discrete-time variable of the algorithm;
- T_s: the sampling time interval;
- $cs[k]$: the charging stage cs at time k;
- $v_{dc}[k]$: the DC voltage measured at k [V];
- $i_{dc}[k]$: the DC current measured at k [A];
- $p_{dc}[k]$: the DC power computed at k [W];
- $\overline{p}_{dc}$[k]: the moving average of p_{dc} computed at k over a time interval of 60 s [W];
- Δp_{dc}[k]: the variation of $\overline{p}_{dc}$ at k observed during a given time interval [W/s];
- $P_{ac}[k]$: the AC active power measured at k [W];
- $\overline{P}_{ac}[k]$: the moving average of P_{ac} computed at k over a time interval of 60 s [W];
- $\Delta P_{ac}[k]$: the variation of $\overline{P}_{ac}$ at k observed during a given time interval [W/s];
- ΔQ: is the cumulative value of the charged capacity during the test [Ah];
- Q_u: is the total usable battery capacity [Ah];

the learning algorithm L_1 used to derive the charging stage cs, the related set of $\underline{\vartheta}$ parameters, and the total usable battery capacity Q_u is described by the flowchart of Fig. 7, where:

$$\Delta p_{dc}[k] = \frac{\overline{p}_{dc}[k] - \overline{p}_{dc}[k-N]}{NT_s}, \tag{3}$$

$$\Delta P_{ac}[k] = \frac{\overline{P}_{ac}[k] - \overline{P}_{ac}[k-N]}{NT_s}, \tag{4}$$

$$\Delta Q[k] = i_{dc}[k]/3600. \tag{5}$$

being N the number of samples in the considered observation window of 60 s.

2) USER SOC MEASUREMENT

Once the value of Q_u has been determined by the learning algorithm L_1, the SoC profile of the battery during the Off-Line full charge test can be determined by applying the following SoC measuring method M implementing the AHC method.

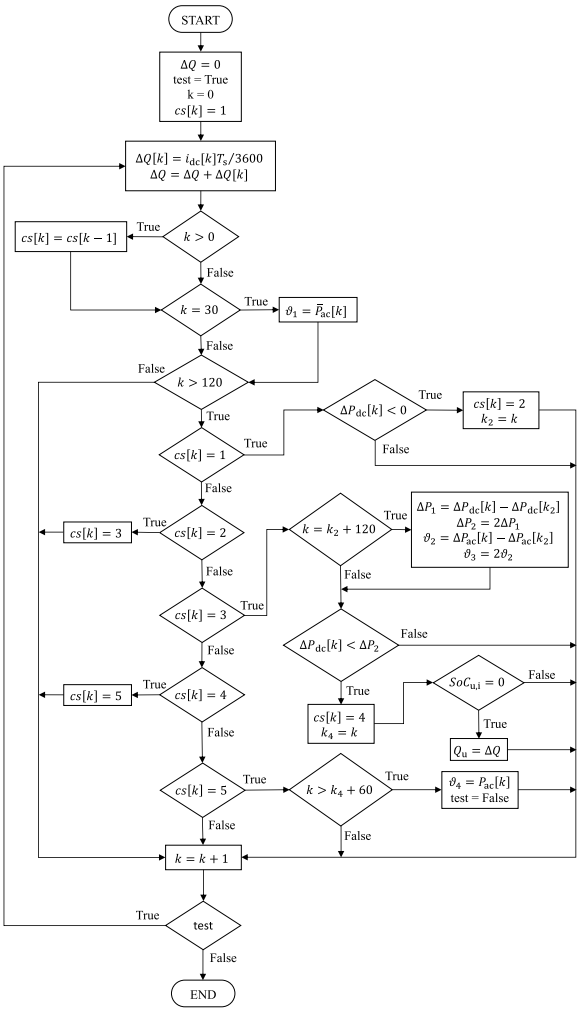

FIGURE 7. Flowchart of the learning algorithm L_1.

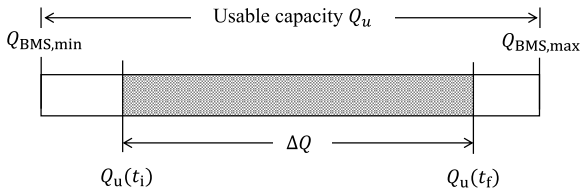

FIGURE 8. Representation of the meaning of the values of $Q_u(t_i)$ and $Q_u(t_f)$.

Assuming that, according to the scheme depicted in Fig. 8, $Q_u(t_i)$ and $Q_u(t_f)$ are the initial and the final capacity of the battery, respectively, the following charge balance equation applies:

$$Q_u(t_f) = Q_u(t_i) + \Delta Q, \tag{6}$$

During the Off-Line full charge test, it is assumed that the initial user state of charge $SoC_{u,i}$ is zero (i.e., $Q_u(t_i) = 0$) and that $Q_u(t_f) = Q_u$ (i.e., the battery undergoes a full charge), thus the usable battery capacity Q_u can be determined by applying Eq. 6. In the case the value of $SoC_{u,i}$ is not known

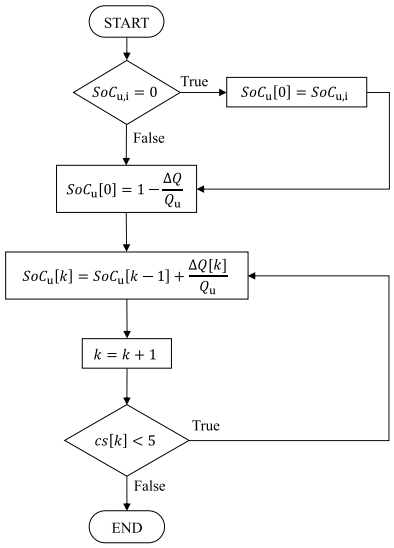

FIGURE 9. Flowchart of the algorithm used to determine the SoC profile.

(as during the validation test of Sections V-B), its value can be determined as follows:

$$SoC_{u,i} = 1 - \frac{\Delta Q}{Q_u}, \tag{7}$$

by using a value of Q_u previously determined in a characterization test executed starting from $SoC_{u,i} = 0$.

Once the value of $SoC_{u,i}$ has been determined, the value of $SoC_u[k]$ can be computed as:

$$SoC_u[k] = SoC_u[k-1] + \frac{\Delta Q[k]}{Q_u}, \tag{8}$$

with $SoC_u[0] = SoC_{u,i}$.

A simple algorithm is then applied to determine the SoC profile, as described by the flowchart depicted in Fig. 9.

3) SoC REGRESSION METHOD

Once the SoC curve $SoC_u[k]$ is determined by implementing the learning algorithm L_1 and the SoC measuring method M, the learning algorithm L_2 is applied to compute the set of regression parameters $\{\underline{\alpha}_{cc}, \underline{\alpha}_{cv}\}$ of $SoC_u[k]$.

As shown in Fig. 10, it has been experimentally noted that the plot of the SoC profile $SoC_u[k]$ against the moving average of the AC active power $\overline{P}_{ac}$ assumes a specific shape formed by two distinct features strongly dependent on the charging mode. During the CC stage, in fact, the power has a monotonically increasing trend, while when the charger operates in CV mode, the active power measured at the input of the battery charger is monotonically decreasing. For this reason, the best fit is a piece-wise linear model that depends on the charging stage $cs[k]$ and can be summarized in the form of Eq. 9:

$$\widehat{SoC}_u[k] = f(\overline{P}_{ac}[k], cs[k]), \tag{9}$$

where $\widehat{SoC}_u[k]$ is the state of charge of the battery obtained from the moving average of the AC active power $\overline{P}_{ac}[k]$ by

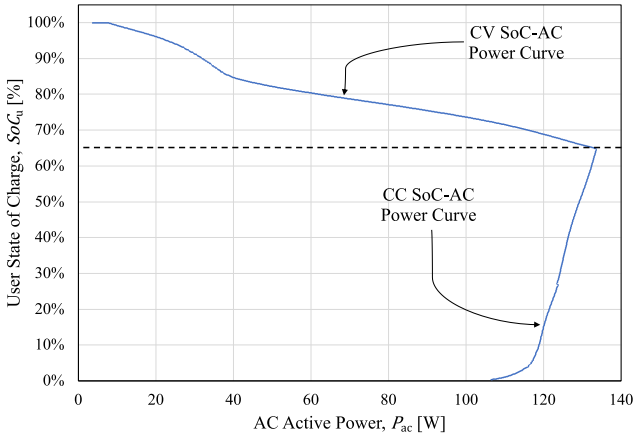

FIGURE 10. Representation of the CC and CV charging curves of $SoC_u[k]$ against the moving average of the AC active power $\overline{P}_{ac}$ during a full charge test.

using a polynomial regression model with f is in the form of a piecewise linear function defined by two seventh-grade equation:

$$f(\overline{P}_{ac}[k], cs[k]) = \begin{cases} f_1(\overline{P}_{ac}[k]) & \text{if } cs[k] = 1, \\ f_3(\overline{P}_{ac}[k]) & \text{if } cs[k] = 3, \end{cases} \tag{10}$$

with:

$$\begin{cases} f_1 = \sum_{n=1}^{7} \alpha_{n,cc} \overline{P}_{ac}[k]^n + \alpha_{0,cc}, \\ f_3 = \sum_{n=1}^{7} \alpha_{n,cv} \overline{P}_{ac}[k]^n + \alpha_{0,cv}. \end{cases} \tag{11}$$

The coefficients $\alpha_{n,cc}$ and $\alpha_{n,cv}$ are obtained by applying a least squares approximation on the set of data classified by L_1 and M.

B. ON-LINE DEPLOYMENT

Once the characterization has been obtained, all the parameters $\underline{\vartheta}$, $\underline{\alpha}_{cc}$, and $\underline{\alpha}_{cv}$ have been learned during the Off-Line test, the estimated charging stage $\widehat{cs}$ and state of charge $\widehat{SoC}_u$ are obtained by using only the moving average of the AC active power $\overline{P}_{ac}[k]$. The algorithm adopted for the estimation of $cs[k]$ and $SoC_u[k]$ is described by the flowchart depicted in Fig. 11, where the two functions f_1 and f_3 for the evaluation of $\widehat{SoC}_u[k]$ have been defined in (10).

IV. MEASUREMENT SETUP

The schematic diagram of the measurement setup adopted during the experiments is depicted in Fig. 12, while the picture of the experimental measurement bench is reported in Fig. 13, where the letters from A to F represent:

- **A**: the AC to DC battery charger;
- **B**: the LEV battery;
- **C**: the AC measurement unit (Fluke 1738 three-phase power quality logger);

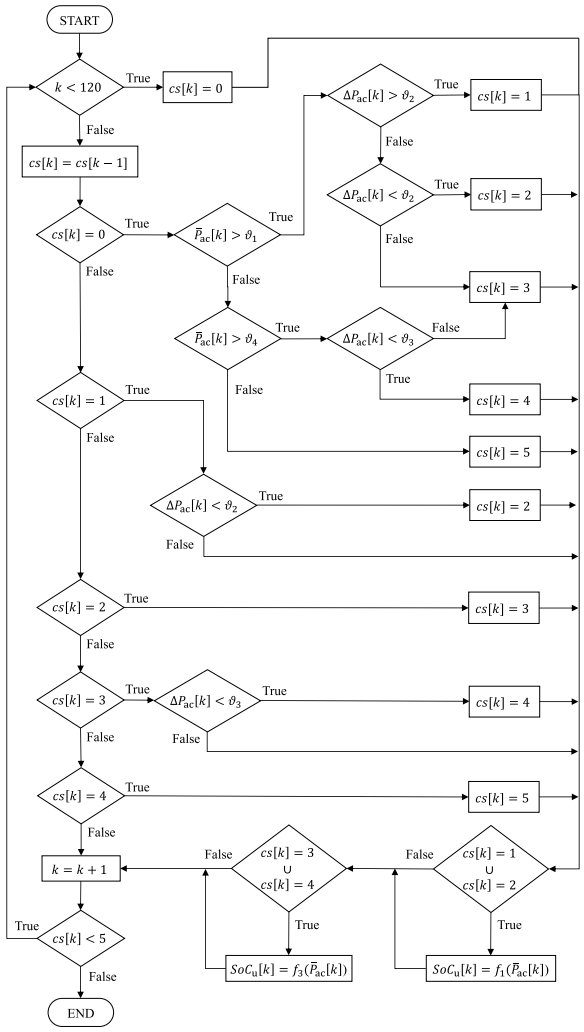

FIGURE 11. Flowchart of the algorithm used for the estimation of $cs[k]$ and $SoC_u[k]$.

- **D**: the DC voltage measurement unit (National Instruments VirtualBench all-in-one instrument);
- **E**: the DC current measurement unit (Agilent 34401A 6 and $\frac{1}{2}$ digits digital multimeter);
- **F**: the Data Acquisition (DAQ) and control computer.

On the DC side, two different instruments have been employed to measure DC voltage and current. The instrument Agilent 34401A (E) is used for measuring the current in series between the AC to DC charger (A) and the battery of the LEV (B). This instrument has a range of 3 A with 6 and $\frac{1}{2}$ digits resolution at a sampling frequency of 6 Sa/s and a shunt resistance of 0.1 Ω in this range. The DC voltage is measured using the digital multimeter function of the all-in-one National Instruments VirtualBench (D), that is 5 and $\frac{1}{2}$ digits digital multimeter with a 100 V.

On the AC side, the power-consumption measurement on the main side of the LEV battery charger A is made with the three-phase power quality logger (C) by using a direct insertion and a current probe (Fluke i40s-EL) with an AC

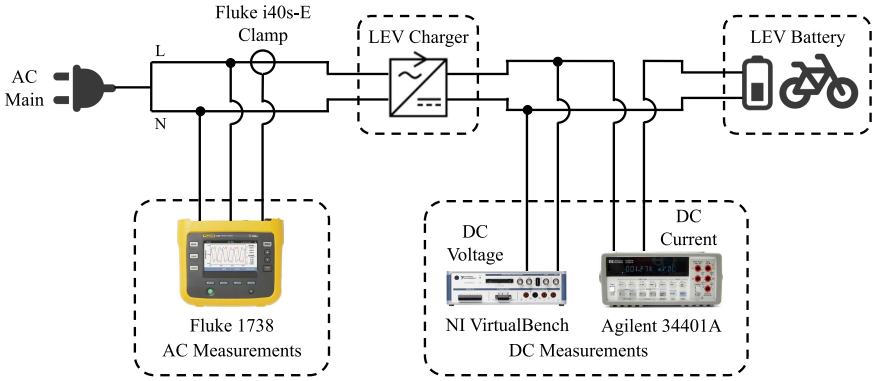

FIGURE 12. Measurement block diagram for the experimental setup.

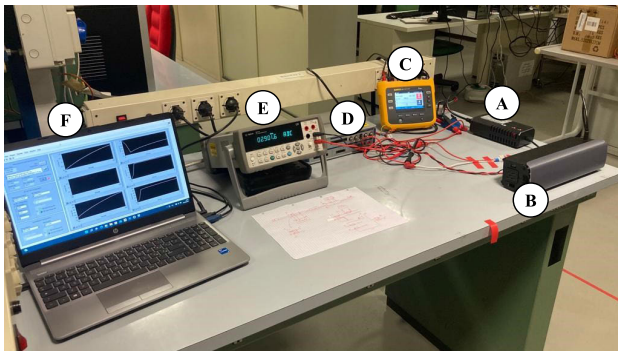

FIGURE 13. Measurement bench.

current clamp with a 4 A and 40 A full-scale ranges for the measurement of the voltage and current, respectively. The AC measurement setup is capable of a voltage resolution of 0.1 V and a current resolution of 1 mA on the 4 A range used during the experiments.

The three instruments are connected to the control computer (D) with different interfaces: USB is used for the National Instrument VirtualBench and Fluke 1738, while IEEE-488 interface is used for the Agilent 34401A multimeter. The computer runs custom software written in National Instrument LabVIEW in order to synchronize the three instruments and collect data. Collected measurements are then processed off-line.

V. EXPERIMENTAL RESULTS

Two different LEV models manufactured by YADEA (referred in the following as "LEV-A" and "LEV-B"), both equipped with a 350 W electric motor, were used to test the proposed method. Each of the LEVs is equipped with the same battery model and provided by the same charger model. The battery model is a *D3614I2* Li-Ion battery manufactured by *DLG*, with a nominal open circuit voltage of 36 V and a rated capacity of 14 A h. The battery charger model is *STC-8108LC* manufactured by *Kunshan ST Electronics*, with a nominal input power of 140 W at 230 V and 50 Hz, and a secondary nominal output of 36 V and 3 A.

Three different experiments was carried out to test and validate the proposed method, namely:

Off-Station Learning Experiment: this experiment represents the implementation of the Off-Line Test for the learning of the $\underline{\vartheta}$, $\underline{\alpha}_{cc}$, and $\underline{\alpha}_{cv}$ parameters that will be used in the On-Line Deployment experiments (i.e., the validation experiments 1 and 2). During the experiment, the "LEV-A" was subjected to a full charge starting from a condition of fully discharged battery. This condition was reached by riding the LEV until the battery was unable to power both the motor and the on-board computer. After the experiment, collected data were used to retrieve the $\underline{\vartheta}$, $\underline{\alpha}_{cc}$, and $\underline{\alpha}_{cv}$ parameters by applying the method described in Section III-A;

Validation Experiment 1: this experiment aims to validate the proposed SoC estimation method when the very same BCS used during the Off-Station learning stage is charged at power outlet. During the experiment, the "LEV-A" was subjected to a full charge starting from a condition of partially discharged battery, with unknown exact SoC. After the experiment, collected AC power measurements are used to compute $\widehat{SoC}_u[k]$ by implementing the algorithm described in Section III-B using the parameters $\underline{\vartheta}$, $\underline{\alpha}_{cc}$, and $\underline{\alpha}_{cv}$ determined during the Off-Station Learning Experiment;

Validation Experiment 2: this experiment aims to validate the proposed SoC estimation when a different BCS of the same family of that used during the Off-Station learning stage is charged at power outlet. During the experiment, the "LEV-B" was subjected to a full charge starting from a condition of fully discharged battery. After the experiment, collected AC power measurements are used to compute $\widehat{SoC}_u[k]$ by implementing the algorithm described in Section III-B, using the parameters $\underline{\vartheta}$, $\underline{\alpha}_{cc}$, and $\underline{\alpha}_{cv}$ determined during the Off-Station Learning Experiment.

The experimental validation of the method is carried out by comparing the values of $\widehat{SoC}_u[k]$ computed by using AC measurements with those computed by applying the L_1 and M algorithms using DC measurements.

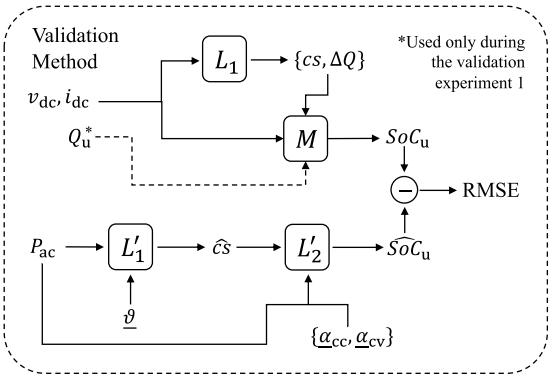

FIGURE 14. Block diagram of the validation method.

An overview of the method adopted during the validation is depicted in the block diagram of Fig. 14. It must be noted that, in the case of the Validation Experiment 1, since the initial SoC was unknown and different from zero, the value of Q_u computed in the Off-Station Learning Experiment was adopted to compute $SoC_u[k]$, being the BCS under test the very same of the learning experiment. Conversely, in the case of the Validation Experiment 2, since the experiment started from a condition of fully discharged battery, the value of Q_u was computed by directly applying the L_1 and M algorithms over the collected DC measurements.

A. OFF-STATION LEARNING EXPERIMENT

As introduced at the beginning of Section V, this experiment implemented the algorithms described in III-A to learn the $\underline{\vartheta}$, $\underline{\alpha}_{cc}$, and $\underline{\alpha}_{cv}$ parameters that will be used in the following validation experiments 1 and 2. During the experiment, the "LEV-A" was subjected to a full charge starting from a condition of fully discharged battery. The experiment lasted more than 10 h (the EoC condition was reached after 9 h, 57 min, and 53 s) and the computed total usable capacity Q_u resulted equal to 13.69 A h, i.e., the 97.8% the nominal battery capacity.

In Fig. 4 the DC voltage and current measurements recorded during the experiment are shown along with the representation of the charging stages, while Fig. 5 shows the moving average of DC power and DC power variations, along with the Δp_1 and Δp_2 power slope thresholds determined by the L_1 algorithm for the identification of the charging stages. Similarly, Fig. 5 shows the moving average of AC power and AC power variations, along with the $\underline{\vartheta}$ parameters determined by the L_1 algorithm. The full list of parameters found by applying L_1 is reported in Table 3.

Once the charging stages have been identified, the user state of charge profile $SoC_u[k]$ was determined by applying the SoC measuring method M, while the set of regression parameters $\{\underline{\alpha}_{cc}, \underline{\alpha}_{cv}\}$ of SoC_u was determined by applying the learning algorithm L_2. The regression parameters $\underline{\alpha}_{cc}$ and $\underline{\alpha}_{cv}$ are reported in Table 4 and Table 5, respectively. The two tables contain the full set of regression coefficients to show the difference of magnitude between the regression functions; moreover, it is worth noting that the computational impact of the seventh-grade regression is limited to off-line characterization experiments, that make use of electronic devices with computational resources of order of magnitude greater than those required by the regression analysis.

In Fig. 15 the moving average of the active power and the computed SoC_u are plotted against the charging time, while in Fig. 16 the interpolated SoC value ($\widehat{SoC}_u$) and

TABLE 3. Charging stage learning results.

Learned parameter	Value
Q_u	13.690 A h
Δp_1	-0.018 W s^{-1}
Δp_2	-0.035 W s^{-1}
CC2CV Time	183.63 min
EoC Time	597.88 min
ϑ_1	106.51 W
ϑ_2	-0.021 W s^{-1}
ϑ_3	-0.035 W s^{-1}
ϑ_4	4.22 W

TABLE 4. SoC regression parameters in CC mode.

Regression parameter	Value
$\alpha_{0,cc}$	-7.38E+02
$\alpha_{1,cc}$	0.00E+00
$\alpha_{2,cc}$	0.00E+00
$\alpha_{3,cc}$	1.46E-02
$\alpha_{4,cc}$	-3.61E-04
$\alpha_{5,cc}$	3.55E-06
$\alpha_{6,cc}$	-1.62E-08
$\alpha_{7,cc}$	2.84E-11

TABLE 5. SoC regression parameters in CV mode.

Regression parameter	Value
$\alpha_{0,cv}$	1.00E+00
$\alpha_{1,cv}$	-5.21E-04
$\alpha_{2,cv}$	7.28E-05
$\alpha_{3,cv}$	-1.37E-05
$\alpha_{4,cv}$	4.15E-07
$\alpha_{5,cv}$	-5.27E-09
$\alpha_{6,cv}$	3.08E-11
$\alpha_{7,cv}$	-6.84E-14

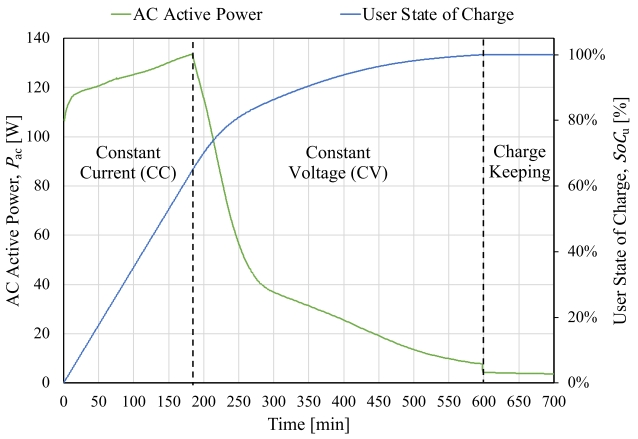

FIGURE 15. Off-Station Learning Experiment. Moving average of the active power and the measured SoC_u.

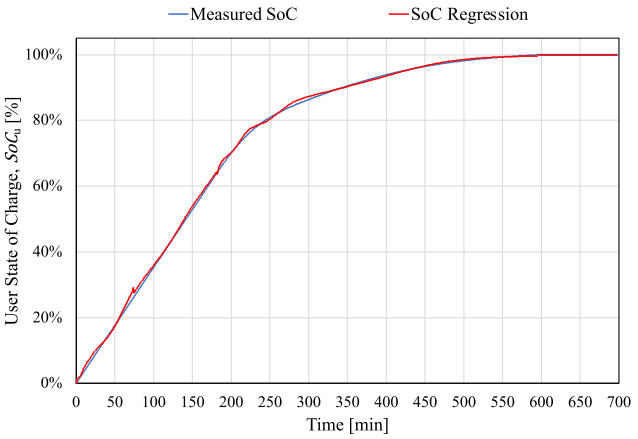

FIGURE 16. Off-Station Learning Experiment. Comparison between the interpolated SoC and the measured SoC values.

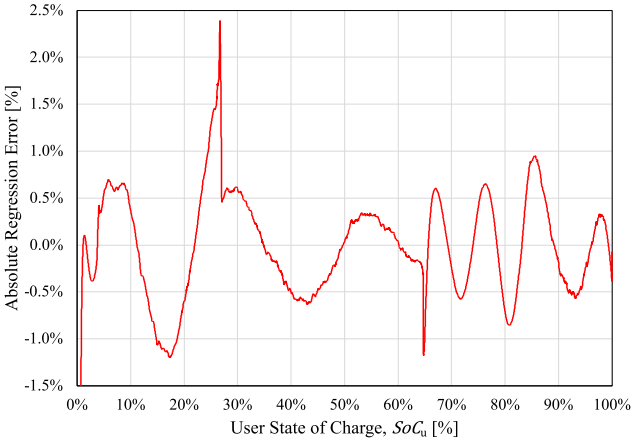

FIGURE 17. Off-Station Learning Experiment. Absolute error of the regression of SoC_u.

the measured SoC value (SoC_u) are compared. Finally, in Fig. 17 the absolute error of the regression is plotted against SoC_u.

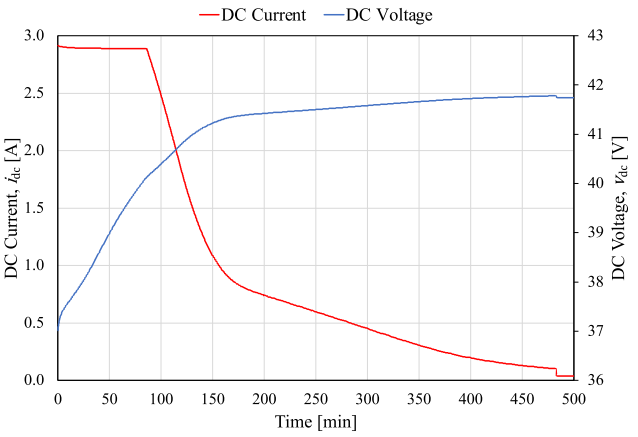

FIGURE 18. Validation Experiment 1. DC current and voltage measurements recorded during the experiment.

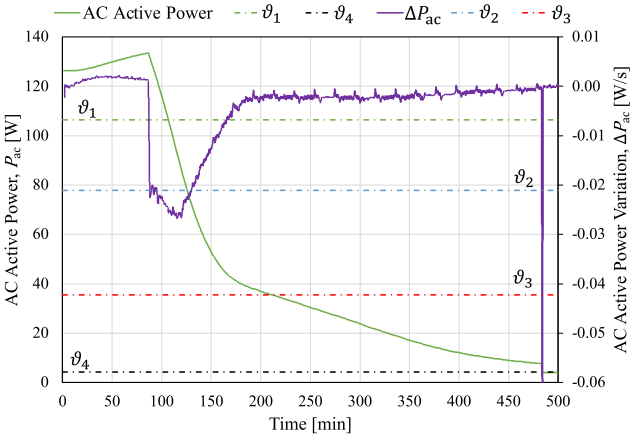

FIGURE 19. Validation Experiment 1. AC power and power variations compared to the $\underline{\vartheta}$ parameters obtained from the Off-Station learning experiment.

B. VALIDATION EXPERIMENT 1

As introduced at the beginning of Section V, during this experiment the "LEV-A" was subjected to a full charge starting from a condition of partially discharged battery, with unknown exact SoC. The experiment lasted more than 8 h (the EoC condition was reached after 8 h, 3 min, and 25 s) and the computed total charged capacity ΔQ resulted equal to 8.62 A h, thus leading to an initial SoC of 37%, computed according to the total usable capacity of 13.69 A h obtained from the Off-Station learning experiment.

In Fig. 18 the DC voltage and current measurements recorded during the experiment are shown, while Fig. 19 shows the moving average of AC power and power variations, along with the $\underline{\vartheta}$ parameters obtained from the Off-Station learning experiment.

The user state of charge profile $SoC_u[k]$ was determined by applying the SoC measuring method M, while collected AC power measurements were used to compute $\widehat{SoC}_u[k]$ by using the parameters obtained from the Off-Station Learning Experiment. Fig. 20 shows the moving average of the AC active power, the estimated SoC, and the measured SoC,

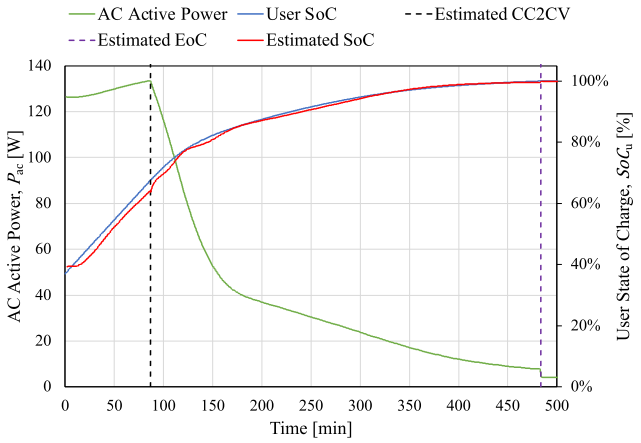

FIGURE 20. Validation Experiment 1. Moving average of the AC active power and comparison between the estimated and measured SoC values, along with the CC2CV and EoC charging states estimated by the L_1' algorithm.

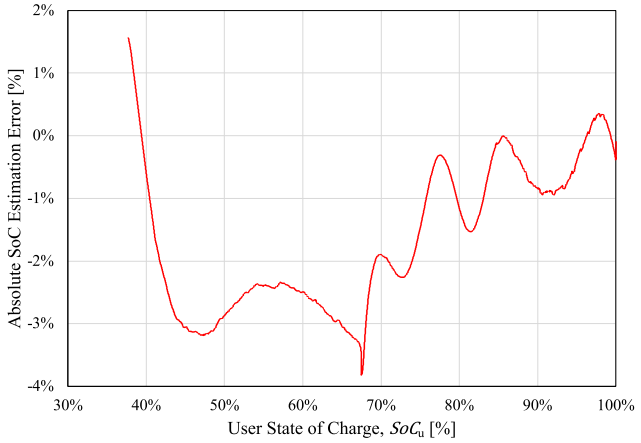

FIGURE 21. Validation Experiment 1. Absolute error of the estimated SoC against the measured SoC.

along with the CC2CV and EoC charging states estimated by the L_1' algorithm. Finally, in Fig. 21 the absolute error of the estimated SoC is plotted against the measured SoC, while in Fig. 22 the absolute error of the estimated SoC is plotted against the charging time.

As it can be observed from the experimental results shown in Fig. 21, the proposed method was able to estimate the SoC of the LEV with an absolute error ranging from -4% to about 1.5%, with a Root Mean Square Error (RMSE) value of 1.26% (computed over all the considered SoC range). The results of the experiment are summarized in Table 6.

C. VALIDATION EXPERIMENT 2

As introduced at the beginning of Section V, during this experiment the "LEV-B" was subjected to a full charge starting from a condition of fully discharged battery. The experiment lasted more than 9 h (the EoC condition was reached after 9 h, 24 min, and 3 s) and the computed a total

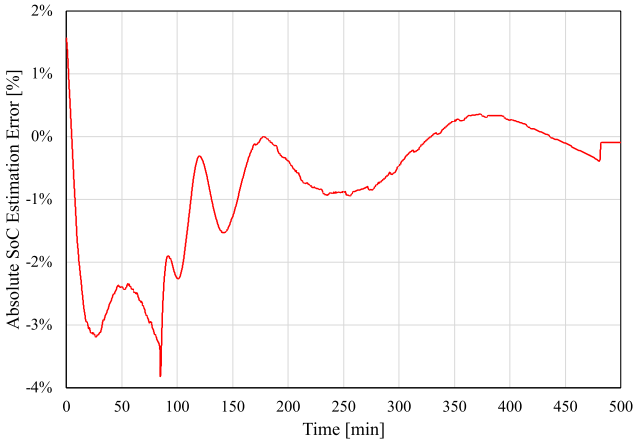

FIGURE 22. Validation Experiment 1. Absolute error of the estimated SoC against the charging time.

TABLE 6. Summary of the results of the Validation Experiment 1.

Indicator	Value
Estimated CC2CV Time	86.48 min
Estimated EoC Time	483.42 min
RMSE of Estimated SoC	1.26 %

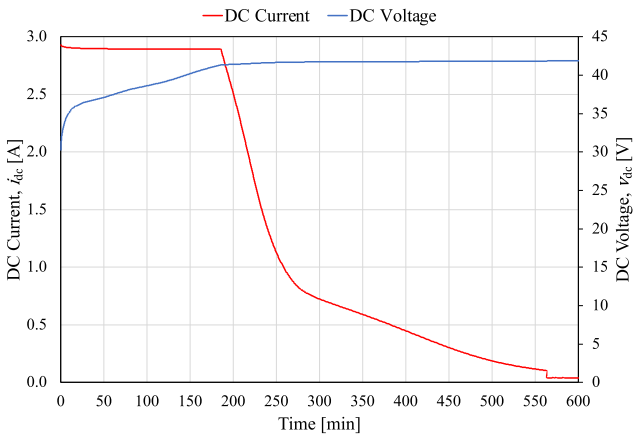

FIGURE 23. Validation Experiment 2. DC current and voltage measurements recorded during the experiment.

usable capacity Q_u of 13.442 A h, i.e., the 96% the nominal battery capacity. It is worth noting that the battery of "LEV-A" showed a total usable capacity equal the 97.8% the rated capacity.

In Fig. 23 the DC voltage and current measurements recorded during the experiment are shown, while Fig. 24 shows the moving average of AC power and power variations, along with the $\underline{\vartheta}$ parameters obtained from the Off-Station learning experiment.

As for the Validation Experiment 1, the user state of charge profile $SoC_u[k]$ was determined by applying the SoC measuring method M, while collected AC power

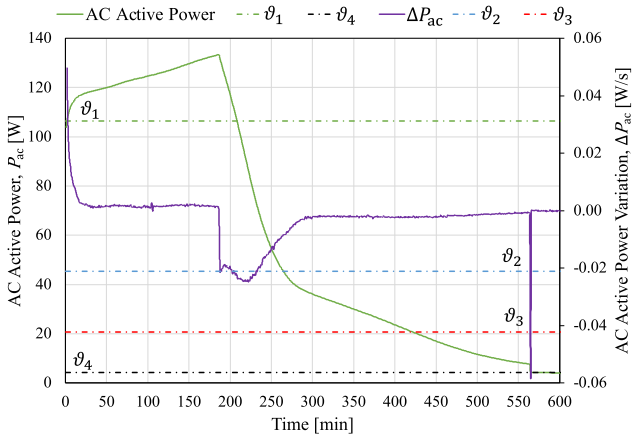

FIGURE 24. Validation Experiment 2. AC power and power variations compared to the $\underline{\vartheta}$ parameters obtained from the Off-Station learning experiment.

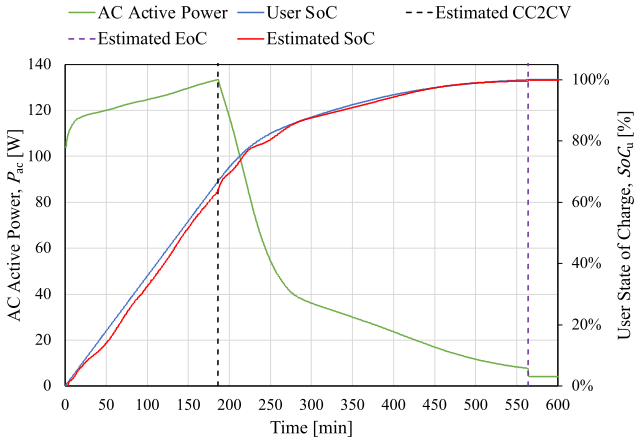

FIGURE 25. Validation Experiment 2. Moving average of the AC active power and comparison between the estimated and measured SoC values, along with the CC2CV and EoC charging states estimated by the L_1' algorithm.

TABLE 7. Summary of the results of the Validation Experiment 2.

Indicator	Value
Estimated CC2CV Time	186.15 min
Estimated EoC Time	564.05 min
RMSE of Estimated SoC	1.54 %

measurements were used to compute $\widehat{SoC}_u[k]$ by using the parameters obtained from the Off-Station Learning Experiment.

Fig. 25 shows the moving average of the AC active power, the estimated SoC, and the measured SoC, along with the CC2CV and EoC charging states estimated by the L_1' algorithm. Finally, in Fig. 26 the absolute error of the estimated SoC is plotted against the measured SoC, while in Fig. 27 the absolute error of the estimated SoC is plotted against the charging time.

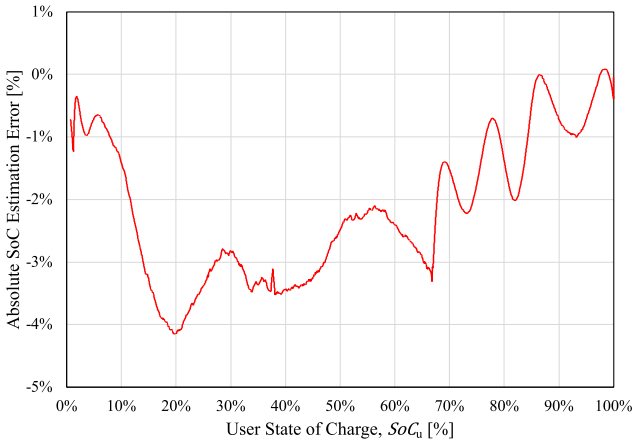

FIGURE 26. Validation Experiment 2. Absolute error of the estimated SoC against the measured SoC.

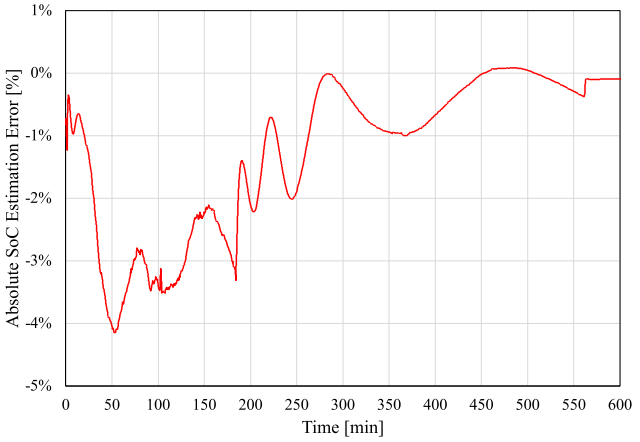

FIGURE 27. Validation Experiment 2. Absolute error of the estimated SoC against the charging time.

As it can be observed from the experimental results shown in Fig. 26, the proposed method was able to estimate the SoC of the LEV with an absolute error ranging from about -4% to about 0%, with an RMSE value of 1.54% (computed over all the considered SoC range). The results of the experiment are summarized in Table 6.

VI. CONCLUSION

The energy required to charge light electric vehicles is increasing as the number of users and related services to smart mobility is growing. Nevertheless, a lack of standardization for e-Bikes and other light electric vehicles remains a problem, and the only common recharging method consists of the use of custom battery chargers connected to alternate current mains. This represents a problem for non Original Equipment Manufacturers that would like to know the charging stage of a connected light electric vehicle. With this in mind, this study presented a method for the identification of the battery charging stage and state of charge based on the measurement of the active power power consumed by the charger.

The proposed method was tested on two different e-Bike models using the same battery and charger models, with the first starting from a condition of partially discharged battery, with an unknown exact state of charge, and the second starting from a condition of fully discharged battery. Two full charge tests were performed, and the state of charge estimated by the proposed approach by using only alternate current active power measurement was compared to that measured by implementing the Coulomb counting method over direct current measurements.

The results of the experiments showed that:

- the proposed method was able to determine the usable state of charge profile of the light electric vehicle batteries with a maximum root-mean-square error (computed over all the usable battery state of charge range) of 1.54%. In particular:
  - i during the partial discharge test, the estimated state of charge accuracy ranged from -4% to about 1.5%, with a root-mean-square error of 1.26%;
  - ii during the full discharge test, the estimated state of charge accuracy ranged from -4% to about 0%, with a root-mean-square error of 1.54%.
- the proposed method could be implemented in electric vehicle charging stations to estimate the real-time state of charge and/or and the expected time of charge of electric vehicles connected to the power outlets, by only using information from pre-tested battery and chargers and data from low-cost smart power meters;

The proposed approach could be successfully applied to light electric vehicle sharing or rent fleets, where the shared/rented vehicles are typically limited to a few models. Indeed, it must be noted that, even though the method can be applied On-Line only for pre-tested vehicles, despite the large number of commercially available light electric vehicles, only a limited set of battery packs (i.e., battery/BMS/charger sets) is available on the market, and most of them are shared among different electric vehicle producers and models.

ACKNOWLEDGMENT

This manuscript reflects only the authors' views and opinions, neither the European Union nor the European Commission can be considered responsible for them.

REFERENCES

[1] S. Will, C. Luger-Bazinger, M. Schmitt, and C. Zankl, "Towards the future of sustainable mobility: Results from a European survey on (electric) powered-two wheelers," *Sustainability*, vol. 13, no. 13, p. 7151, Jun. 2021.

[2] (May 2022). *Global EV outlook 2022*. Paris. Accessed: April 2023. [Online]. Available: https://www.iea.org/reports/global-ev-outlook-2022

[3] J. Leijon and C. Boström, "Charging electric vehicles today and in the future," *World Electr. Vehicle J.*, vol. 13, no. 8, p. 139, Jul. 2022.

[4] H. S. Das, M. M. Rahman, S. Li, and C. W. Tan, "Electric vehicles standards, charging infrastructure, and impact on grid integration: A technological review," *Renew. Sustain. Energy Rev.*, vol. 120, Mar. 2020, Art. no. 109618.

[5] S. Sachan, S. Deb, and S. N. Singh, "Different charging infrastructures along with smart charging strategies for electric vehicles," *Sustain. Cities Soc.*, vol. 60, Sep. 2020, Art. no. 102238.

[6] G. R. Mouli, P. Vanduijsen, T. Velzeboer, G. Nair, Y. Zhao, A. Jamodkar, O. Isabella, S. Silvester, P. Bauer, and M. Zeman, "Solar powered e-bike charging station with AC, DC and contactless charging," in *Proc. 20th Eur. Conf. Power Electron. Appl. (EPE ECCE Europe)*, Sep. 2018, pp. P.1–P.10.

[7] S. Rinaldi, M. Pasetti, A. Flammini, and G. Maternini, "Multimodal electric vehicle supply equipment: Toward a sustainable and resilient mobility," in *Proc. IEEE Int. Workshop Metrol. Automot. (MetroAutomotive)*, Jul. 2021, pp. 243–247.

[8] M. Pasetti, M. Longo, S. Rinaldi, P. Ferrari, E. Sisinni, and A. Flammini, "On the sustainable charging of electric vehicles in the presence of distributed photovoltaic generation," in *Proc. IEEE Sustain. Power Energy Conf. (iSPEC)*, Dec. 2022, pp. 1–5.

[9] *Electric Vehicle Conductive Charging System—Part 1: General Requirements*, Standard IEC 61851-1, International Electrotechnical Commission (IEC), Geneva, Switzerland, Feb. 2017.

[10] N. Kularatna and K. Gunawardane, "Rechargeable battery technologies: An electronic circuit designer's viewpoint," in *Energy Storage Devices for Renewable Energy-Based Systems*, 2nd ed. Boston, MA, USA: Academic Press, 2021, pp. 65–98.

[11] F. Mohammadi, "Lithium-ion battery state-of-charge estimation based on an improved Coulomb-Counting algorithm and uncertainty evaluation," *J. Energy Storage*, vol. 48, Apr. 2022, Art. no. 104061.

[12] A. Seaman, T.-S. Dao, and J. McPhee, "A survey of mathematics-based equivalent-circuit and electrochemical battery models for hybrid and electric vehicle simulation," *J. Power Sources*, vol. 256, pp. 410–423, Jun. 2014.

[13] X. Li, C. Wu, C. Fu, S. Zheng, and J. Tian, "State characterization of lithium-ion battery based on ultrasonic guided wave scanning," *Energies*, vol. 15, no. 16, p. 6027, Aug. 2022.

[14] J.-J. Chang, X.-F. Zeng, and T.-L. Wan, "Real-time measurement of lithium-ion batteries' state-of-charge based on air-coupled ultrasound," *AIP Adv.*, vol. 9, no. 8, Aug. 2019, Art. no. 085116.

[15] E. Galiounas, T. G. Tranter, R. E. Owen, J. B. Robinson, P. R. Shearing, and D. J. L. Brett, "Battery state-of-charge estimation using machine learning analysis of ultrasonic signatures," *Energy AI*, vol. 10, Nov. 2022, Art. no. 100188.

[16] S. Nejad, D. T. Gladwin, and D. A. Stone, "A systematic review of lumped-parameter equivalent circuit models for real-time estimation of lithium-ion battery states," *J. Power Sources*, vol. 316, pp. 183–196, Jun. 2016.

[17] X. Han, M. Ouyang, L. Lu, and J. Li, "Simplification of physics-based electrochemical model for lithium ion battery on electric vehicle. Part I: Diffusion simplification and single particle model," *J. Power Sources*, vol. 278, pp. 802–813, Mar. 2015.

[18] X. Han, M. Ouyang, L. Lu, and J. Li, "Simplification of physics-based electrochemical model for lithium ion battery on electric vehicle. Part II: Pseudo-two-dimensional model simplification and state of charge estimation," *J. Power Sources*, vol. 278, pp. 814–825, Mar. 2015.

[19] N. Meddings, M. Heinrich, F. Overney, J.-S. Lee, V. Ruiz, E. Napolitano, S. Seitz, G. Hinds, R. Raccichini, M. Gaberšček, and J. Park, "Application of electrochemical impedance spectroscopy to commercial Li-ion cells: A review," *J. Power Sources*, vol. 480, Dec. 2020, Art. no. 228742. [Online]. Available: https://www.sciencedirect.com/science/article/pii/S0378775320310466

[20] K. Luo, X. Chen, H. Zheng, and Z. Shi, "A review of deep learning approach to predicting the state of health and state of charge of lithium-ion batteries," *J. Energy Chem.*, vol. 74, pp. 159–173, Nov. 2022.

[21] Q. Yu, Y. Huang, A. Tang, C. Wang, and W. Shen, "OCV-SOC-temperature relationship construction and state of charge estimation for a series–parallel lithium-ion battery pack," *IEEE Trans. Intell. Transp. Syst.*, vol. 24, no. 6, pp. 6362–6371, Jun. 2023.

[22] Q.-Q. Yu, R. Xiong, L.-Y. Wang, and C. Lin, "A comparative study on open circuit voltage models for lithium-ion batteries," *Chin. J. Mech. Eng.*, vol. 31, no. 1, p. 65, Aug. 2018.

[23] X. Dang, L. Yan, K. Xu, X. Wu, H. Jiang, and H. Sun, "Open-circuit voltage-based state of charge estimation of lithium-ion battery using dual neural network fusion battery model," *Electrochimica Acta*, vol. 188, pp. 356–366, Jan. 2016.

[24] L. Shen, J. Li, L. Zuo, L. Zhu, and H. T. Shen, "Source-free cross-domain state of charge estimation of lithium-ion batteries at different ambient temperatures," *IEEE Trans. Power Electron.*, vol. 38, no. 6, pp. 6851–6862, Jun. 2023.

[25] G. Patrizi, B. Picano, M. Catelani, R. Fantacci, and L. Ciani, "Validation of RUL estimation method for battery prognostic under different fast-charging conditions," in *Proc. IEEE Int. Instrum. Meas. Technol. Conf. (I2MTC)*, May 2022, pp. 1–6.
[26] J. Hong, H. Zhang, and X. Xu, "Thermal fault prognosis of lithium-ion batteries in real-world electric vehicles using self-attention mechanism networks," *Appl. Thermal Eng.*, vol. 226, May 2023, Art. no. 120304.
[27] M. Hossain, M. E. Haque, and M. T. Arif, "Kalman filtering techniques for the online model parameters and state of charge estimation of the Li-ion batteries: A comparative analysis," *J. Energy Storage*, vol. 51, Jul. 2022, Art. no. 104174.
[28] L. Hu, R. Hu, Z. Ma, and W. Jiang, "State of charge estimation and evaluation of lithium battery using Kalman filter algorithms," *Materials*, vol. 15, no. 24, p. 8744, Dec. 2022.
[29] P. Nian, Z. Shuzhi, and Z. Xiongwen, "Co-estimation for capacity and state of charge for lithium-ion batteries using improved adaptive extended Kalman filter," *J. Energy Storage*, vol. 40, Aug. 2021, Art. no. 102559.
[30] W. Zhang, L. Wang, L. Wang, C. Liao, and Y. Zhang, "Joint state-of-charge and state-of-available-power estimation based on the online parameter identification of lithium-ion battery model," *IEEE Trans. Ind. Electron.*, vol. 69, no. 4, pp. 3677–3688, Apr. 2022.
[31] M. Catelani, L. Ciani, R. Fantacci, G. Patrizi, and B. Picano, "Remaining useful life estimation for prognostics of lithium-ion batteries based on recurrent neural network," *IEEE Trans. Instrum. Meas.*, vol. 70, pp. 1–11, 2021.
[32] B. Tar and A. Fayed, "An overview of the fundamentals of battery chargers," in *Proc. IEEE 59th Int. Midwest Symp. Circuits Syst. (MWSCAS)*, Oct. 2016, pp. 1–4.
[33] M. Brenna, F. Foiadelli, C. Leone, and M. Longo, "Electric vehicles charging technology review and optimal size estimation," *J. Electr. Eng. Technol.*, vol. 15, no. 6, pp. 2539–2552, Nov. 2020.
[34] G. R. C. Mouli, P. Van Duijsen, F. Grazian, A. Jamodkar, P. Bauer, and O. Isabella, "Sustainable e-bike charging station that enables AC, DC and wireless charging from solar energy," *Energies*, vol. 13, no. 14, p. 3549, Jul. 2020.
[35] S. Mesentean, W. Feucht, A. Mittnacht, and H. Frank, "Scheduling methods for smart charging of electric bikes from a grid-connected photovoltaic-system," in *Proc. UKSim 5th Eur. Symp. Comput. Modeling Simulation*, Nov. 2011, pp. 299–304.
[36] F. Hipolito, C. A. Vandet, and J. Rich, "Charging, steady-state SoC and energy storage distributions for EV fleets," *Appl. Energy*, vol. 317, Jul. 2022, Art. no. 119065.
[37] S. Mesentean, W. Feucht, H.-G. Kula, and H. Frank, "Smart charging of electric scooters for home to work and home to education transports from grid connected photovoltaic-systems," in *Proc. IEEE Int. Energy Conf.*, Dec. 2010, pp. 73–78.

MARCO PASETTI (Member, IEEE) received the M.Sc. degree in industrial engineering and the Ph.D. degree in mechanical engineering from the University of Brescia, Brescia, Italy, in 2008 and 2013, respectively. He is currently an Assistant Professor in electrical energy systems with the Department of Information Engineering, University of Brescia. His current research interests include energy systems, distributed generation, renewable energy sources, photovoltaics, energy storage, demand-side management, electric vehicles charging systems, energy management systems, supervisory control and data acquisition, and smart grids.

SALVATORE DELLO IACONO (Member, IEEE) received the B.Sc. and M.Sc. degrees in electronic engineering and the Ph.D. degree in industrial engineering from the University of Salerno, Italy, in 2014, 2018, and 2022, respectively. He is currently a Research Fellow with the Department of Information Engineering, University of Brescia, Italy. He carried out researches on inertial measurement systems and positioning algorithms; he is actively involved in embedded systems development, power management systems, and smart metering. His research interests include industrial control systems, embedded real time signal processing on microcontrollers and DSPs, and IIoT devices.

DARIO ZANINELLI (Senior Member, IEEE) received the Ph.D. degree in electrical engineering from Politecnico di Milano, in 1989. He is currently a Full Professor with the Department of Energy, Politecnico di Milano. His research interests include power system harmonics and power system analysis. He is a member of AEI and the Italian National Research Council Group of Electrical Power System.

Open Access funding provided by 'Università degli Studi di Brescia' within the CRUI CARE Agreement